

# Mineral–Melt Equilibria in a Hydrous Basaltic System: Computer Modeling

R. R. Al'meev\* and A. A. Ariskin\*\*

\* *Geological Department, Moscow State University (MGU), Vorob'evy gory, Moscow, 119899 Russia*

\*\* *Vernadsky Institute of Geochemistry and Analytical Chemistry,  
Russian Academy of Sciences, ul. Kosygina 19, Moscow, 117975 Russia*

Received December 12, 1995

**Abstract**—A method is proposed for using experimental data on phase equilibria in igneous rocks to develop a computer model of basalt magma crystallization under hydrous conditions. The approach includes: (1) the development of an empirical relation for the calculation of water solubility in basalt, andesite, and granite melt as a function of composition, temperature, and pressure; (2) estimating on the basis of this relation the water concentration in quench glasses produced in experiments on the melting of rocks under water-saturated conditions; (3) calculation of correction coefficients accounting for the various water effects on the liquidus temperature of main mineral phases in the basaltic system; and (4) development of an algorithm for the modeling of basalt magma crystallization on the basis of the obtained relations. With the modified “hydrous” version of the COMAGMAT software, phase equilibrium calculations for a high-alumina basaltic melt at  $P_{\text{H}_2\text{O}} = 2$  kbar well reproduce the experimental data on the composition of water-saturated melts, equilibrium temperature, and the proportion of crystallizing minerals.

## INTRODUCTION

Numerical simulations of phase equilibria in magmatic systems have been widely used in petrological and geochemical investigations since the 1980s. By using a computer, the partial melting of mantle peridotites and trends of crystallization, temperature, and geochemical evolution of magmas in volcanic centers and intrusive chambers, for instance [1–4], can be calculated. Computer programs were designed for modeling diverse open (assimilation and mixing) and closed (intrusive chambers) magmatic systems; their common feature is an algorithm for the calculation of phase equilibria under given external conditions.

These computer models generally include empirical data on the melting of natural samples and synthetic mixtures under the conditions of fixed temperature, pressure, and oxygen fugacity. This information includes a considerable body of data on the composition of coexisting solid phases and melts, which can be mathematically processed to find relations on the equilibrium distribution of components in a mineral–melt system [2, 4] or to calculate the thermodynamic functions of major phases of the igneous system [3]. These equations (geothermometers) and functions compose the *thermodynamic basis* to calculate equilibria between a magmatic melt and one or more mineral phases. Using the algorithms that were developed on the basis of these relations, phase equilibria were at first calculated for mineral–melt associations. Further progress in computer modeling of melting and crystal-

lization will involve their application to a broader range of compositions and conditions.

Today, one of the main problems is related to the fact that most existing computer models are currently restricted to “dry” systems and do not account for the influence of volatile components on the evolution of igneous melts. Thus, the development of an effective method to take into account the presence of  $\text{H}_2\text{O}$  in the system is an important challenge in theoretical petrology, because water is the main volatile component that controls the displacement of cotectics and evolution of the liquid in modeling magma crystallization. This problem is complicated mainly not by mathematical formulation or the development of a specific algorithm, but rather by the uncertainty and, in most cases, by the lack of direct experimental data on melt–water interactions in the petrologically important silicate system.

In this work we propose a simple method to take into account the  $\text{H}_2\text{O}$  influence on phase equilibria that does not yet involve all aspects of silicate melt–water interactions or a particular mechanism of water dissolution. Our approach includes the development of an empirical equation for water solubility in basic and felsic melts, an estimation of  $\text{H}_2\text{O}$  contents in water-saturated experimental glasses, and a calculation on this basis of the correction coefficients to determine the liquidus temperature of major rock-forming minerals at a given  $\text{H}_2\text{O}$  concentration in a melt. The incorporation of these coefficients into an algorithm for crystallization temperature calculation for main rock-forming minerals (COMAGMAT software [4]) will allow us to

account, as a first approximation, for the influence of H<sub>2</sub>O on phase equilibria, because the difference in the correction coefficients for various minerals implies that the sequence of mineral appearance on the liquidus may change in the transition from dry to hydrous conditions.

The efficiency of the proposed method was demonstrated by modeling phase equilibria in the magnesian and aluminous basalts of the Klyuchevskoi volcano [5]. This study has shown that the presence of approximately 2 wt % H<sub>2</sub>O in the initial magma was the main factor controlling the formation of high-alumina evolved liquids, which were formed via polybaric fractionation at a depth interval of 60–20 km.

#### METHOD TO ACCOUNT FOR THE INFLUENCE OF H<sub>2</sub>O ON CRYSTALLIZATION TEMPERATURE

The equilibrium between solid phase and melt in water-free systems is determined by COMAGMAT for a given pressure and crystal fraction, when the equilibrium temperature  $T_{\text{dry}}$ , is not known beforehand, but determined during the calculation. With this algorithm, an equilibrium mineral assemblage is selected based on a certain formalization of a common application of phase diagrams under the assumption that the equilibrium of each mineral phase with the melt is topologically characterized by a liquidus surface, which is determined over the whole range of compositions (Fig. 1) [6]. Thus, for a given melt composition, each mineral phase, *A* and *B*, for example, may be characterized by a respective liquidus temperature  $T^i$  ( $T^A$  or  $T^B$ ), and the equilibrium is stable only for the phase (or association) with the higher  $T^i$  (in the case of the dry system on Fig. 1, this is  $T_{\text{dry}}^B$ ). This is the criterion to determine mineral phases occurring in the equilibrium state.

Liquidus temperatures of various minerals are depressed to varying degrees by the water dissolved in the melt; as a result, a mineral association equilibrated with a water-bearing melt may differ from that formed under dry conditions (phase *A* in the case of the hydrous system in Fig. 1). For instance, the experiments of Yoder and Tilley [7] with typical tholeiitic basalt at different water pressures demonstrated that olivine, pyroxene, and plagioclase appear in the same order at any water pressure: olivine and pyroxene were always the first to crystallize. However, the crystallization of high-alumina basalt started with plagioclase at low  $P_{\text{H}_2\text{O}}$ , whereas it was the last crystalline phase to appear at a water pressure of more than 2000 bar [7].

The depression of the liquidus temperature for main rock-forming minerals can be accounted for by introducing a correction in the procedure of phase equilibrium calculation:

$$T_{\text{hydr}}^i = T_{\text{dry}}^i - \lambda^i C_{\text{H}_2\text{O}}, \quad (1)$$

where  $T_{\text{hydr}}^i$  and  $T_{\text{dry}}^i$  are the temperatures of mineral *i* appearance on the liquidus in the hydrous and dry systems, respectively;  $C_{\text{H}_2\text{O}}$  is the concentration of water in the melt; and  $\lambda^i$  (°C /%H<sub>2</sub>O) is the coefficient equal to the depression of the liquidus temperature of mineral *i* due to the increase of water content in the melt by 1 wt %, which depends on  $P_{\text{H}_2\text{O}}$  (see discussion below).

This coefficient is the only unknown parameter in equation (1), because the crystallization temperature of mineral *i* in the dry system is calculated by COMAGMAT and the concentration of dissolved water and total pressure are the input parameters of the model. Thus, the value of  $\lambda^i$  for olivine, plagioclase, orthopyroxene, and clinopyroxene may be obtained from the experimental data on phase equilibria in synthetic and natural systems under water-saturated conditions:

$$\lambda^i = (T_{\text{dry}}^i - T_{\text{hydr}}^i) / C_{\text{H}_2\text{O}}. \quad (2)$$

Let us assume that the association olivine (*Ol*)–glass (*L*)<sup>1</sup> was produced in an experiment on the melting of a natural olivine basalt under water-saturated conditions.

Then,  $T_{\text{hydr}}^{\text{Ol}}$  is the experimental temperature,  $T_{\text{dry}}^{\text{Ol}}$  as a function of melt composition may be calculated by *Ol* geothermometers [4], and  $C_{\text{H}_2\text{O}}$  is the concentration of H<sub>2</sub>O in quench glass (wt %) measured by experiment or calculated. The coefficient  $\lambda^{\text{Ol}}$  equals the depression of the olivine liquidus temperature due to the increase of water concentration by 1 wt % for the particular experiment under the experimental pressure. By processing a series of experimental data on the equilibrium *Ol*–*L*, one can calculate the average value of the coefficient  $\lambda^{\text{Ol}}$  as a function of  $P_{\text{H}_2\text{O}}$ . This approach is illustrated by the scheme of liquidus relationships in the melt of olivine basalt under dry and water-saturated conditions shown in Fig. 2.

Obviously, similar calculations may be carried out for other main phases of the basaltic system.

#### EXPERIMENTAL DATA

The INFOREX database was used to solve the problem. Its last version, INFOREX-3.0 [8], includes the results of 162 experimental works on phase equilibria in natural and synthetic systems that were published during 1962–1995. The database comprises comprehensive information on the conditions of 6174 experiments and includes 8311 compositions of coexisting phases, including approximately 3200 quench glasses. The data can be sorted by the type of system under study (basalts, andesites, norites, etc.), presence or absence of volatile components, pressure, temperature,

<sup>1</sup> Phase notation: *Ol*, olivine; *Pl*, plagioclase; *Aug*, augite; *Opx*, orthopyroxene; *Pig*, pigeonite; *Cpx*, clinopyroxene; *Qtz*, quartz; *Mt*, magnetite; and *L*, melt (quench glass).

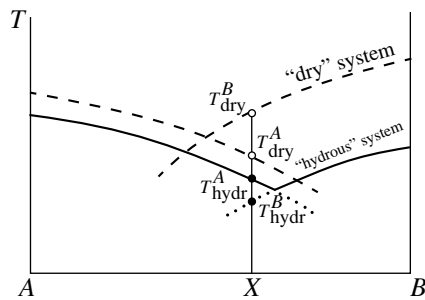


**Fig. 1.** Schematic liquidus relations in binary "dry" and "hydrous" systems. The addition of water into the system results in the change of the crystallization order of minerals *A* and *B* because of the different effect of water on the liquidus temperature of the phases.

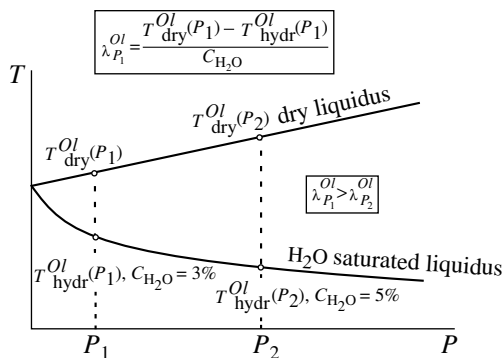


**Fig. 2.** Schematic  $P$ - $T$  diagram of liquidus relations under dry and water-saturated conditions at a pressure up to 10 kbar for the melt of hypothetical olivine basalt. This diagram illustrates the method of calculation and the meaning of correction coefficients  $\lambda^i$  in equation (2):  $\lambda^{Oe}$  values are calculated at a given pressure as a difference between the temperatures of dry and water-saturated liquidus normalized by the concentration of water in the saturated melt.

oxygen fugacity, run duration, container type, composition of quench glass, and resulting phase association. After filtration with respect to the experimental conditions, the user can select a specific equilibrium and create files with the compositions of the coexisting phases at given external conditions directly from the INFOREX environment. The processes of search and file formation take from 5–10 s to several minutes on a PC that is AT-386 class or better; this program is, therefore, a powerful petrological tool for analyzing and using experimental data.

Currently, INFOREX includes 1618 experiments on water-saturated phase equilibria. In this data set, the compositions of quench glasses are available only for 461 experiments from 24 works; in some cases the compositions of equilibrium minerals are reported. These works used natural samples (basalts, andesites, dacites, lherzolites, rhyolites, etc.) and synthetic mixtures under  $H_2O$ -saturated conditions at temperatures

of 675 to 1300°C, pressures of 100 bar to 30 kbar, and run durations of 1 to 816 h. The processing of these data is complicated by the fact that, except for a few works [9–11], the concentration of  $H_2O$  in melt (glass) corresponding to saturation conditions (presence of fluid phase) is not known in these experiments. Thus, the development of a function relation for accurately predicting water solubility in silicate melts is of particular importance.

## ESTIMATES OF WATER SOLUBILITY

As was already noted,  $H_2O$  concentration in quench glass (melts) was not directly measured in the majority of studies on equilibrium phase relations under water-saturated conditions, although attempts to estimate  $C_{H_2O}$  were made repeatedly. Some works estimated  $H_2O$  concentrations as the departure of the totals in the analyses of experimental glasses from 100 wt % [9];  $H_2O$  contents were calculated using the modified Burnham [10] model; and some authors applied the Stolper [11, 12] model. In this respect, of interest are the results of Sisson and Grove [13], who determined  $H_2O$  contents by IR spectroscopy in quench glasses from three experiments and compared them with the values obtained using the Burnham [14] model and the method of Housh and Luhr [15] (Table 1). The measured and calculated values of  $C_{H_2O}$  obtained by these authors appeared to be comparable. It is worth noting that the Stolper [11, 16] model (see below) underestimated  $H_2O$  contents by 0.5–1.5 wt % for the same compositions (Table 1).

In this work we developed and applied an empirical equation to calculate water concentration in experimental glasses. Our decision to not use the approaches of Burnham or Stolper was justified, first, by the internal inconsistencies in these thermodynamic models, which have been repeatedly discussed in the literature; and, second, by the ambiguity in some equilibrium constants and specific parameters. We will discuss below some of the problems with the application of the Burnham and Stolper models.

### Burnham Model

The model was formulated more than 20 years ago and is based on direct  $P$ - $V$ - $T$  measurements for a hydrous albite melt. Its essence is as follows. Burnham and Davis proposed an empirical relation for the water partial molar volume in an albite melt for temperatures of 700 to 950°C and pressures of 3 to 8.5 kbar using the least-square method and their own experimental data [17]. Using these equations and the experimental results on water solubility in an albite melt, they calculated the values of the thermodynamic functions (chemical potential, fugacity, and activity) for water in an albite

**Table 1.** Comparing H<sub>2</sub>O concentrations in quench experimental glasses from natural samples with calculated values

Sample [13]	T, °C	P, bar	H <sub>2</sub> O in melt				
			IR	I	II	III	IV
1140 MF#18	1054	1000	3.76	3.4	4	3.28	3.59
81-T-116	1050	2000	6.17	5.07	5.84	4.69	5.95
87S35A#5	985	2000	5.94	5.2	5.81	4.47	5.33

Note: IR, infrared spectrometry of experimental quench glasses [13]; the calculated values are for the model of (I) Burnham [14], (II) Housh and Luhr [15], (III) Stolper [11, 16], and (IV) equation (13). 1140MF#18, andesite; 81-T-116, hornblende high-alumina basaltic andesite, and 87S35A#5, aluminous hornblende gabbro.

melt as a function of its mole fraction ( $X_{\text{H}_2\text{O}}^L$ ) [18, 19]. On the basis of these relations (the activity of water dissolved in the melt  $a_{\text{H}_2\text{O}}^L$  as a function of  $X_{\text{H}_2\text{O}}^L$ ) and the experimental data on the viscosity and electric conductivity of a hydrous albite melt, Burnham proposed a mechanism for H<sub>2</sub>O dissolution in an albite melt [14] and demonstrated the linear dependence of  $a_{\text{H}_2\text{O}}^L$  on  $(X_{\text{H}_2\text{O}}^L)^2$  at  $X_{\text{H}_2\text{O}}^L < 0.5$  (Figs. 1–5 in [19]):

$$a_{\text{H}_2\text{O}}^L = k(X_{\text{H}_2\text{O}}^L)^2, \quad (3)$$

and positive deviations from this relationship at  $X_{\text{H}_2\text{O}}^L > 0.5$ :

$$a_{\text{H}_2\text{O}}^L = 0.25k \exp[(6.52 - 2667/T)(X_{\text{H}_2\text{O}}^L - 0.5)]. \quad (4)$$

In Burnham's opinion, the quantity  $k$  in equations (2) and (3) is analogous to the constant in Henry's law for a dissociated solution. Assuming that the vapor phase was pure water ( $a_{\text{H}_2\text{O}}^L = 1$ ), Burnham calculated the values of  $k$  as a function of temperature and pressure (Fig. 16.3 in [14]). The equation for calculating  $k$  was obtained by the least-square technique and first published by Burnham in one of the most recent works devoted to the model [20] ( $P$ , bar;  $T$ , K):

$$\begin{aligned} \ln k = & 5.00 + (\ln P)(4.481 \times 10^{-8} T^2 \\ & - 1.51 \times 10^{-4} T - 1.137) + (\ln P)^2(1.831 \times 10^{-8} T^2 \\ & - 4.882 \times 10^{-5} T + 4.656 \times 10^{-2}) \\ & + 7.80 \times 10^{-3} (\ln P)^3 - 5.012 \times 10^{-4} (\ln P)^4 \\ & + T(4.754 \times 10^{-3} - 1.621 \times 10^{-6} T). \end{aligned} \quad (5)$$

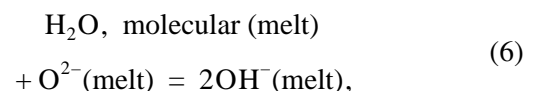
The values of  $k$  and equations (2) and (3) are used to estimate water solubility in the albite melt for certain intensive variables [14]. In addition, Burnham demonstrated that after normalizing the melt composition to eight atoms of oxygen (equivalent to the albite formula) the water solubility becomes essentially the same for a

wide range of melt compositions. This allowed the practical use of this model to estimate  $C_{\text{H}_2\text{O}}$  in experimental glasses for a given pressure and temperature.

Although widely used by petrologists, the Burnham model was repeatedly subject to criticism, for instance [21–24]. First, the experimental values of the partial molar volume of water in an albite melt were obtained at water concentrations of 8.25 and 10.9 wt %, and were extrapolated to lower pressures and water concentrations; therefore, the estimates of  $C_{\text{H}_2\text{O}}$  at  $X_{\text{H}_2\text{O}}^L < 0.5$  should be regarded with caution [24]. Second, several authors believe that the scheme proposed by Burnham for H<sub>2</sub>O solubility in aluminosilicate melts is not internally consistent [21–23]. It should be noted also that the calculated values of  $C_{\text{H}_2\text{O}}$  at high pressures (3–4 kbar and higher) are systematically underestimated, especially for andesite melts (Fig. 3, Table 1).

#### Stolper Model

Proceeding from data on the structural position of water in glasses obtained by Raman spectroscopy, IR spectroscopy, and NMR, Stolper proposed an alternative thermodynamic model for water solubility in aluminosilicate melts [16]. This research demonstrated varying concentrations of molecular H<sub>2</sub>O and hydroxyl ion OH<sup>-</sup> depending on the net water content in the system. It was found that, at H<sub>2</sub>O contents in the system below 2–3.5 wt % (depending on melt composition), water occurs in the melt predominantly in hydroxyl form. As the bulk concentration of water increases (>4 wt %), molecular water becomes predominant, whereas the hydroxyl concentration remains constant. On the basis of this data, Stolper considered two reactions of water interaction with water-saturated silicate melt:



and



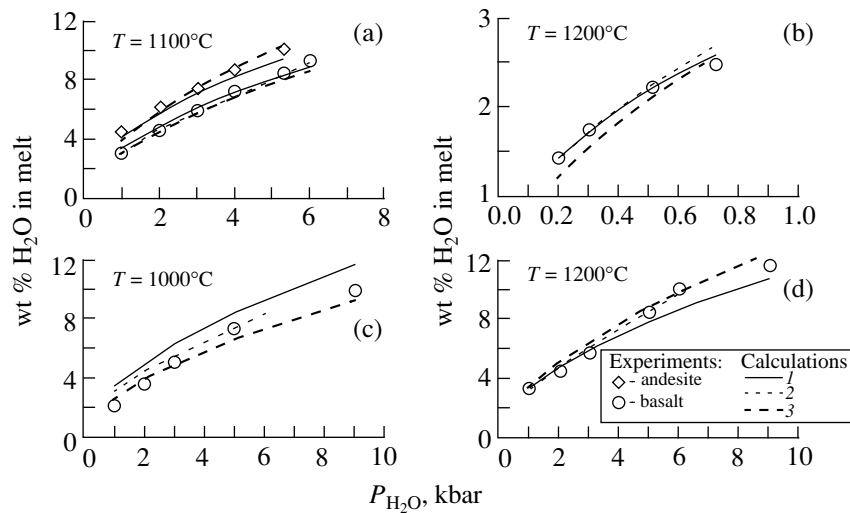


**Fig. 3.** Experimental and model isotherms of H<sub>2</sub>O solubility in natural silicate melts. Experiments: (a) Mount Hood andesite and Columbia River basalt [26]; (b) mid-ocean ridge basalt [11]; (c) and (d) Kirgurich basalt [27]. Calculations: (1) Burnham model [14]; (2) Stolper model [11, 16]; (3) empirical equation (13). Note. The values of water solubility in the melts of Mount Hood andesite and Columbia River basalt calculated by the Stolper model are practically identical.

whose equilibrium constants are:

$$K_1 = \frac{(a_{\text{OH}}^L)^2}{(a_{\text{O}}^L)(a_{\text{H}_2\text{O}}^L)}, \quad (8)$$

$$K_2 = \frac{a_{\text{H}_2\text{O}}^L}{a_{\text{H}_2\text{O}}^V} = \frac{X_{\text{H}_2\text{O}}^L}{f_{\text{H}_2\text{O}}/f_{\text{H}_2\text{O}}^0}, \quad (9)$$

respectively, where  $a_{\text{H}_2\text{O}}^L$  and  $a_{\text{H}_2\text{O}}^V$  are the activities of water in the melt and the equilibrium vapor phase;  $f_{\text{H}_2\text{O}}$  is the water fugacity in vapor phase; and  $f_{\text{H}_2\text{O}}^0$  is the water fugacity in the vapor phase under standard conditions. Using the formalism of the regular solution model, Stolper *et al.* [25] deduced a relation between different forms of H<sub>2</sub>O dissolved in melt:

$$-\ln \left[ \frac{(X_{\text{OH}}^L)^2}{(X_{\text{H}_2\text{O}}^L)(1 - X_{\text{OH}}^L - X_{\text{H}_2\text{O}}^L)} \right] = A + BX_{\text{OH}}^L + CX_{\text{H}_2\text{O}}^L, \quad (10)$$

where  $X_{\text{OH}}^L$  and  $X_{\text{H}_2\text{O}}^L$  are the mole fractions of the hydroxyl ion and molecular water in the melt; and  $A$ ,  $B$ , and  $C$  are the functions of the equilibrium constant  $K_1$  and interaction parameters of species in the water-saturated melt. The values of these coefficients were obtained by the least-square method from experimental data on the concentrations of H<sub>2</sub>O and OH<sup>-</sup> in albite melt.

Using the relation for H<sub>2</sub>O activity in the water-saturated melt at constant temperature  $T^0$ :

$$a_{\text{H}_2\text{O}}^L(P, T^0) = a_{\text{H}_2\text{O}}^{L,0}(P^0, T^0) \frac{f_{\text{H}_2\text{O}}(P, T^0)}{f_{\text{H}_2\text{O}}^0(P^0, T^0)} \times \exp \left[ \frac{-V_{\text{H}_2\text{O}}^L(P - P^0)}{RT^0} \right], \quad (11)$$

where  $V_{\text{H}_2\text{O}}^L$  is the molar volume of water in the melt, and the approximation of Henry's law ( $a_{\text{H}_2\text{O}}^L \cong X_{\text{H}_2\text{O}}^L$ ) and the modified Redlich-Kwong equation (for  $f_{\text{H}_2\text{O}}$  calculation), one can determine the molar fraction of molecular water, and using equation (10), the molar fraction of hydroxyl ion dissolved in the melt.

This approach was applied recently to calculate the concentrations of dissolved H<sub>2</sub>O in molecular and hydroxyl forms in a basaltic melt at a pressure of 200–5000 bar and a temperature of 1200°C [11]. For the coefficients  $A$ ,  $B$ , and  $C$  we used (equation (10)) the values 0.403, 15.333, and 10.894, respectively, obtained for an albite melt; the value of partial molar volume of water in melt was taken as  $V_{\text{H}_2\text{O}}^L = 12 \text{ cm}^3/\text{mol}$ ; and the mole weight of basalt normalized to one oxygen atom, 36.594. We also calculated  $C_{\text{H}_2\text{O}}$  by the Stolper method for a series of natural melts using the model parameters listed above (Fig. 3). The calculation illustrated good agreement with experimental data for all compositions but the melt of Stone Mountain andesite [26]. The calculations have shown that the

value of  $C_{\text{H}_2\text{O}}$  obtained by the Stolper method is not sensitive to melt composition: the values of water concentration for basaltic and more felsic melts (for instance, andesitic) were almost equal, which is not consistent with experimental observations [27]. Some other assumptions of the model are also ambiguous, for example the constancy of the partial molar volume of water in the melt. The experimental investigation of the albite system did demonstrate that this quantity depends on temperature and pressure [17]; large variations of  $V_{\text{H}_2\text{O}}^L$  were observed between the albite melt and rhyolite (see review in [28]).

It should be noted that, strictly speaking, the Stolper model is not a method of  $C_{\text{H}_2\text{O}}$  estimation and is used mainly to describe the behavior of different forms of  $\text{H}_2\text{O}$  as a function of bulk water concentration in the system. Holloway and Blank [12] believe that the Stolper method may be used to calculate the water concentration only for those melts for which direct spectroscopic measurements were carried out.

#### *Empirical Equation of Water Solubility*

An alternative approach to finding the most accurate calculation of water content in experimental glasses is to use the empirical dependency of  $C_{\text{H}_2\text{O}}$  on composition, pressure, and temperature, which may be developed by the least-square method applied directly to experimental data.

Critical for such an approach is the possibility that the derived equation may be used only within the limited composition range corresponding to the input conditions. However, taking into account that direct measurements of  $\text{H}_2\text{O}$  solubility are available for a variety of melt compositions, we believe that such a model may be applied to systems ranging from basalts to granites. An attractive feature of the empirical approach is that it uses direct results under experimental conditions and does not invoke additional (sometimes problematic) information on the thermodynamic properties of  $\text{H}_2\text{O}$  in systems with other compositions.

The database on  $\text{H}_2\text{O}$  solubility includes the results of 79 experiments that were carried out in the field of two-phase melt–vapor equilibrium over the pressure interval of 200 bar–9 kbar and at temperatures of 800–1200°C [11, 13, 26, 27]. The representative data set includes experiments with the melts of Mount Hood andesite, Columbia River basalt ( $N = 11$ ,  $1 < P < 6$  kbar,  $t = 1100^\circ\text{C}$ ) [26], Kirgurich basalt ( $N = 14$ ,  $1 < P < 9$  kbar,  $1000 < t < 1200^\circ\text{C}$ ) [27], El'dzhurtin granite ( $N = 49$ ,  $1000 < P < 3500$  bar,  $800 < t < 1300^\circ\text{C}$ ) [27], mid-ocean ridge basalt ( $N = 4$ ,  $200 < P < 1000$  bar,  $t = 1200^\circ\text{C}$ ) [11], and high-alumina basalt ( $N = 1$ ,  $P = 2000$  bar,  $t = 1054^\circ\text{C}$ ) [13].

The experimental data were approximated by the linear model:

$$\ln C_{\text{H}_2\text{O}} = a + b/T + c \ln P + d\phi, \quad (12)$$

where, in addition to pressure and temperature, various structural chemical parameters of the melt  $\phi$ , such as Si/O, (Si + Al)/O, Al/Si, Si/Mg, (Na + K)/Al, etc., are used as independent variables of linear regression. The reproducibility of experimental data was tested by the solution of the inverse problem for pressure and temperature. We tried approximately 30 variants with different combinations of the structural chemical parameters of the melt; the experimental data appeared to be best described (with an average deviation of ~0.3 wt %  $\text{H}_2\text{O}$ ) by the following equation:

$$\begin{aligned} \ln C_{\text{H}_2\text{O}} = & (4.39 \pm 1.50) \\ & + [(38438.3 \pm 5402.4)\text{Si/O} \\ & - (14710.2 \pm 2142.9)]/T + (0.59 \pm 0.01) \ln P \\ & - (21.45 \pm 3.80)\text{Si/O} + (3.89 \pm 0.69)\text{Al/Si}, \end{aligned} \quad (13)$$

where temperature is in Kelvin; pressure, in bars; and melt composition parameters, in atom fractions.

The coefficient at inverse temperature, (38438.3 Si/O – 14710.2) in equation (13) accounts for the experimentally determined difference in the character of the temperature dependency of water solubility in basaltic and granitic melts [27]. It was found that the system basalt–water is characterized by a positive temperature coefficient of  $\text{H}_2\text{O}$  solubility, whereas in the system granite–water, the  $\text{H}_2\text{O}$  solubility decreases with increasing temperature up to a pressure of approximately 3500 bar and increases at higher pressures. Recently, the occurrence of a temperature minimum on a water-saturated surface was confirmed in the system orthoclase–albite–quartz [29].

Figure 4 shows the calculated and experimental values of  $\text{H}_2\text{O}$  solubility in basalt, andesite, and granite melts and the example of the inverse problem solution for pressure. The fact that accuracy of calculations—0.3 wt %  $\text{H}_2\text{O}$ —is comparable with experimental uncertainties and in agreement with the values calculated by the Burnham and Stolper models (Table 1, Fig. 3) shows that equation (13) can be reliably used to calculate  $\text{H}_2\text{O}$  solubility in basalt and andesite melts up to a pressure of 10 kbar.

#### H<sub>2</sub>O EFFECT ON THE LIQUIDUS TEMPERATURES OF MAIN ROCK-FORMING MINERALS

Using the search procedure of INFOREX-3.0 [8], we selected runs from the bulk of water-saturated experiments with samples of lherzolites, basalts, and andesites at a pressure of up to 10 kbar. The compositions of quench glasses from these experiments were grouped by the presence of a particular mineral in the equilibrium mineral association (for example, for oliv-

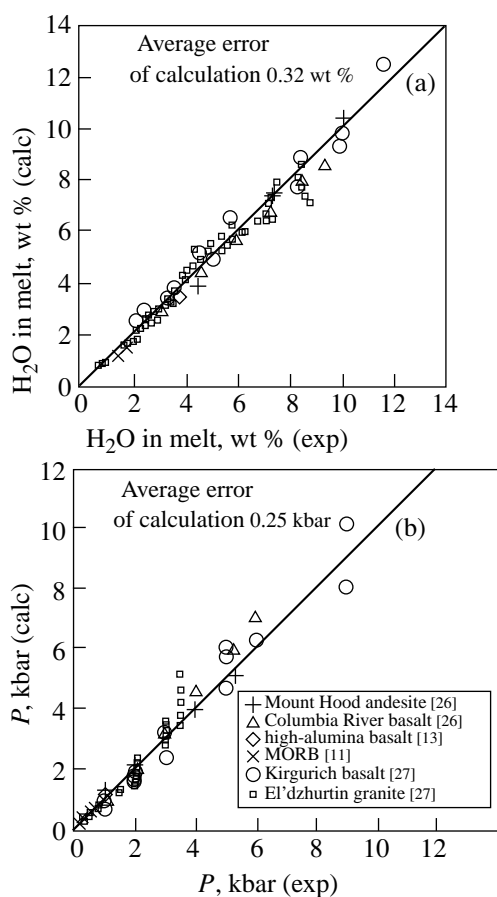


**Fig. 4.** Experimental and calculated values of  $H_2O$  solubility (a) and total pressure  $P = P_{H_2O}$  (b) for given temperature and composition. The calculations were carried out using empirical equation (13).

ine such associations included  $Ol + L$ ,  $Ol + Pl + L$ ,  $Ol + Aug + Pl + L$ , etc.). Thus, four data sets were produced: *olivine-liquid* (69 experiments), *plagioclase-liquid* (81), *augite-liquid* (56), and *orthopyroxene-liquid* (19). Crystallization temperatures were calculated for the compositions of all quench glasses under dry conditions ( $T_{dry}^i$ ) and experimental pressures using the COMAGMAT program complex. The calculated values appeared to be 100–300°C higher than the respective experimental temperatures ( $T_{hydr}^i$ ), which resulted evidently from  $H_2O$  depressing the liquidus temperature of minerals.

For each experiment, the difference between  $T_{dry}^i$  and  $T_{hydr}^i$  was then normalized with respect to  $H_2O$  concentration (see equation (2)), which was calculated by empirical equation (13). The calculated average values of the degree of crystallization temperature depression  $\lambda^i$  for olivine, plagioclase, augite, and orthopyrox-

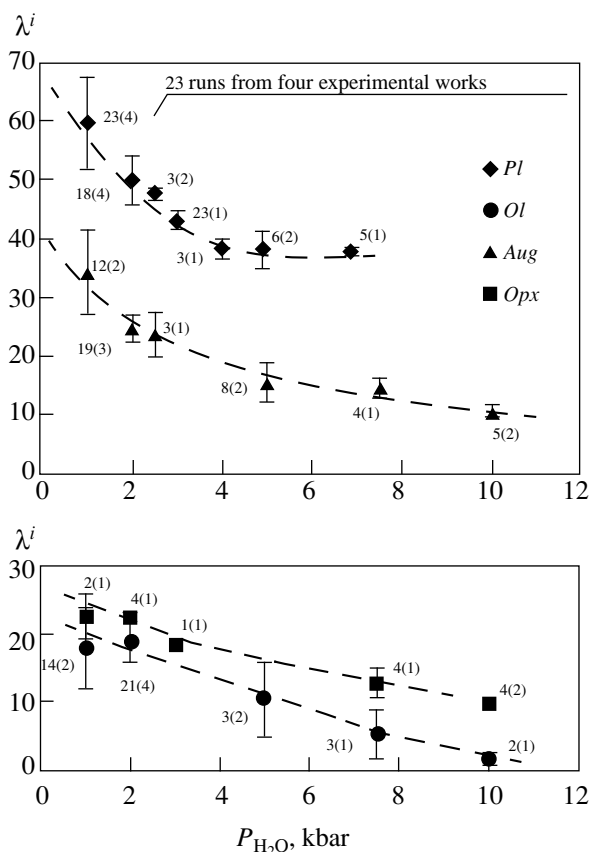


**Fig. 5.** Average values of the correction coefficients  $\lambda_i$  as a function of total pressure  $P = P_{H_2O}$ :  $Ol$ ,  $Aug$ ,  $Opx$ ,  $Pl$  (Table 2); the coefficients  $\lambda^i$  were calculated by equations (2) and (13) and characterize the depression of liquidus temperature of a mineral normalized to 1 wt % of water in melt.

ene as a function of pressure  $P = P_{H_2O}$  are shown in Table 2 and Fig. 5.

The results allow us to formulate two main conclusions concerning water influence on the crystallization temperature of silicate minerals: (1) the effect of  $H_2O$  dissolved in melt declines regularly in the order  $Pl \Rightarrow Aug \Rightarrow Opx \Rightarrow Ol$  and (2) for each mineral the value of  $\lambda^i$  decreases regularly with increasing pressure (Fig. 5). The first conclusion concurs with the well-known concepts of the influence of water on the crystallization temperatures of femic minerals and plagioclase and quantitatively characterizes this effect for use in petrological analysis (Table 2). For example, Yoder and Tilley [7] observed in experiments on the melting of basalt that at  $P_{H_2O} = 2000$  bar that the plagioclase liquidus temperature decreased by more than 200°C, whereas for femic minerals this effect was only around 100°C for the same water pressure [7]. Assuming that  $H_2O$  solubility in a basalt melt at  $P_{H_2O} = 2000$  bar is approximately 5–6 wt % [30], one can calculate the depression of liquidus temperatures under these condi-

**Table 2.** Correction coefficients  $\lambda^i$  ( $^{\circ}\text{C}$  per 1 wt %  $\text{H}_2\text{O}$ ) for main rock-forming minerals as a function of pressure  $P = P_{\text{H}_2\text{O}}$  in the system

$P$ , kbar	$\lambda^{Ol}$	$\lambda^{Aug}$	$\lambda^{Opx}$	$\lambda^{Pl}$
1	$17.9 \pm 6.0$	$34.3 \pm 7.1$	$22.4 \pm 3.4$	$59.6 \pm 7.8$
2	$18.7 \pm 2.9$	$24.8 \pm 2.2$	$22.3 \pm 1.2$	$49.9 \pm 4.2$
2.5		$23.7 \pm 3.9$		$47.6 \pm 1.0$
3			18.3	$43.1 \pm 1.5$
4				$38.3 \pm 1.6$
5	$10.2 \pm 5.5$	$15.5 \pm 3.3$		$38.1 \pm 3.1$
6.9				$37.8 \pm 0.6$
7.5	$5.1 \pm 3.7$	$14.5 \pm 1.6$	$12.5 \pm 2.2$	
10	$1.3 \pm 0.7$	$10.5 \pm 1.1$	$9.3 \pm 1.0$	

tions using Table 2 or Fig. 4 diagrams for all minerals, multiplying water concentrations by the respective coefficient  $\lambda^i$  at a given pressure. Such a calculation shows that the liquidus temperature will decrease by 250–300 $^{\circ}\text{C}$  for plagioclase; 125–150 $^{\circ}\text{C}$  for augite; and 100–120 $^{\circ}\text{C}$  for olivine and orthopyroxene, which is consistent with the experimental results [7]. The difference in the degree of depression of crystallization tem-

perature for plagioclase and feric minerals results in differently increasing solubilities for the quartz–feldspar and iron–magnesium components of the melt in the presence of  $\text{H}_2\text{O}$ , which was also noted in [31].

The second result is not so apparent and is better substantiated for plagioclase than for feric minerals, which are represented in Fig. 5 by only 2–5 points at high pressures. In spite of the apparently regular change in  $\lambda^i$  values for each mineral with pressure, it cannot be ruled out that this stems from the inaccuracy of liquidus temperature  $T_{\text{dry}}^i$  calculation at high pressures by COMAGMAT [4] and of estimates of water solubility  $C_{\text{H}_2\text{O}}$  at high values of  $P = P_{\text{H}_2\text{O}}$  by equation (13). However, we emphasize this conclusion, because the pressure dependency of  $\lambda^i$  is potentially important for petrological interpretations. This problem evidently requires further experimental study.

### PHASE EQUILIBRIUM MODELING IN THE PRESENCE OF $\text{H}_2\text{O}$

The approach outlined above was applied for modeling phase equilibria under hydrous conditions. We calculated liquid lines of descent for a high-alumina basalt for which experimentally studied phase relations and compositions of quench glasses were reported using the modified “hydrous” version of COMAGMAT [4, 5]. We used for comparison the experimental data of

**Table 3.** Comparing experimental [30] and calculated equilibrium temperatures and melt compositions for high-alumina basalt at varying crystal fractions under water-saturated conditions,  $P = P_{\text{H}_2\text{O}} = 2$  kbar

Phase association	$Ol + Mt + L$		$Ol + Pl + Aug + Mt + L$		$Ol + Pl + Aug + Mt + L$		$Ol + Pl + Aug + Mt + L$		Initial composition of high-alumina basalt [30]	
	run no.	#6	Model	#4	Model	#11	Model	#12		Model
crystals, %	7	7	6.00	14	11.50	19	17.00	49	47.00	
$T$ , $^{\circ}\text{C}$	1050	1050	1058	1050	1050	1035	1046	1000	1022	
$\text{SiO}_2$	48.20	48.20	48.80	49.40	49.32	49.00	49.61	52.50	51.98	48.20
$\text{TiO}_2$	0.65	0.65	0.71	0.72	0.60	0.72	0.54	0.98	0.21	0.66
$\text{Al}_2\text{O}_3$	19.40	19.40	19.46	19.20	19.56	19.70	19.81	19.20	20.83	18.20
$\text{FeO}$	8.37	8.37	8.09	8.28	7.72	8.69	7.63	8.04	6.94	8.39
$\text{MnO}$	0.16	0.16	0.15	0.15	0.17	0.16	0.17	0.20	0.19	0.16
$\text{MgO}$	6.96	6.96	7.37	6.58	7.10	6.37	6.96	4.99	5.76	9.89
$\text{CaO}$	13.20	13.20	12.83	12.60	12.84	12.10	12.45	9.64	10.18	12.01
$\text{Na}_2\text{O}$	2.89	2.89	2.45	2.77	2.55	3.08	2.70	4.15	3.74	2.29
$\text{K}_2\text{O}$	0.12	0.12	0.10	0.12	0.10	0.11	0.11	0.21	0.17	0.09
$\text{P}_2\text{O}_5$	0.09	0.09	0.05	0.06	0.06	0.09	0.06	0.14	0.10	0.05
$\text{H}_2\text{O}$ , calc.	–	–	5.98	–	5.98	–	6.05	–	6.27	–

Note: The calculations were carried out using the COMAGMAT software for the initial composition shown in the table. The calculations started from water undersaturated conditions: for run #6, 5.6 wt %  $\text{H}_2\text{O}$ ; #4, 5.3 wt %  $\text{H}_2\text{O}$ ; #11, 5.0 wt %  $\text{H}_2\text{O}$ ; and #12, 3.3 wt %  $\text{H}_2\text{O}$ . The columns of model compositions show melts saturated with  $\text{H}_2\text{O}$  calculated by equation (13).

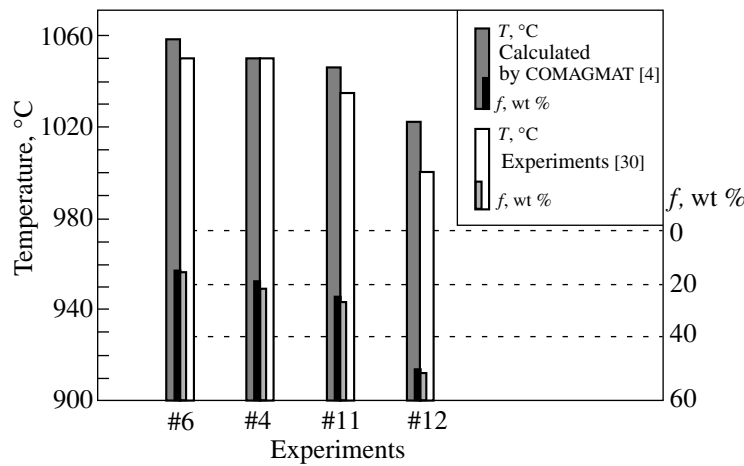


**Fig. 6.** Experimental and calculated equilibrium temperatures for water-saturated high-alumina basalt at a given crystal content  $f$  (wt %). Phase associations and melt compositions are shown in Table 3.

Sisson and Grove [30] on the melting of high-alumina basalt (sample 79–35 g) under water-saturated conditions at a total pressure of  $P = 2000$  bar. The concentration of  $H_2O$  in the experimental glasses was not measured; however, the authors estimated it as 6 wt % on the basis of their previous results [30]. The experimental results are shown in Table 3, the phase composition of liquidus association and composition of quench glasses are defined by the equilibrium temperature and the degree of crystallization (see triangles on Fig. 7).

We attempted to quantitatively model this experiment, i.e., to calculate the phase proportions and the composition of a water-saturated melt under a given degree of crystallization in the system [32]. For this purpose, corrections similar to those of equation (1) were incorporated into the COMAGMAT procedure of temperature calculation accounting for the depression of mineral crystallization temperatures in the presence of water. The following values of  $\lambda^i$  were used ( $^{\circ}C$  per 1 wt %  $H_2O$ ): *Ol*, 17.5; *Pl*, 45.0; *Aug*, 19.5. These values lie within the confidence intervals of  $\lambda^i$  at  $P = 2$  kbar (Table 2) and agree with the results of modeling the formation conditions of high-alumina basalts from the Klyuchevskoi volcano [5].

Saturation conditions during the partial crystallization of a high-alumina basalt melt were modeled in the following way. Certain amounts of water (2.0, 2.1, 2.2 wt %  $H_2O$ , etc.) were added to an initial composition (Table 3), and the normal cycle of batch crystallization was carried out using COMAGMAT [4] in each of these systems at a crystal fraction increment of  $\Delta f = 1\%$ . The calculations were performed at  $P = 2$  kbar and under redox conditions corresponding to those of the quartz–fayalite–magnetite buffer [30]. It was assumed that water behaved as an incompatible component during crystallization and its concentration in the melt increased continuously. The concentration of  $H_2O$  cannot obviously exceed a certain limiting value (solubility), and following each  $j$ th step of crystallization the

model concentration  $C_{H_2O}^{mod(j)}$  was compared with water solubility  $C_{H_2O}^{(j)}$  calculated by equation (13). If the condition  $C_{H_2O}^{mod(j)} < C_{H_2O}^{(j)}$  was fulfilled, the saturation was not achieved and the calculations proceeded, otherwise, at  $C_{H_2O}^{mod(j)} \geq C_{H_2O}^{(j)}$  the calculations terminated and the value of  $C_{H_2O}^{(j)}$  was taken as the  $H_2O$  solubility at a given crystal fraction  $f^j$ .

In such way, for each series of calculations with varying initial water contents, the equilibrium parameters of the system melt–minerals–vapor were determined including crystal fraction in the system  $f^j$ , equilibrium temperature  $T^j$ , mineral proportions on the liquidus, and the composition of liquid. The analysis of this information demonstrated that some  $f^j - T^j$  pairs are similar to the results obtained in experiments #6, #4, #11, and #12 (Fig. 6) and the model  $H_2O$  solubilities appeared to be close to 6 wt % (Table 3), the value suggested by Sisson and Grove [30]. This may be regarded as evidence that our computer model is realistic.

In this context, it is interesting to compare the compositions of the experimental and model water-saturated melts. As Table 3 shows, the agreement is rather convincing for most components ( $SiO_2$ ,  $Al_2O_3$ ,  $MgO$ ,  $CaO_2$ , and  $Na_2O$ ). The deviations in  $FeO$  and  $TiO_2$  probably result from inaccuracies of the thermodynamic model used to compute titanomagnetite crystallization [4]. Figure 7 shows the experimental (triangles) and model (crosses) compositions of the water-saturated melts projected onto the pseudoternary *Ol–Cpx–Qtz* and *Ol–Pl–Cpx* diagrams. Also shown are the experimental compositions of cotectic melts (*Ol + Pl + Aug + Mt + Pig*) at a pressure of 1 atm under dry conditions (data from INFOREX [8]). This diagram illustrates that the calculations faithfully reproduce the dis-

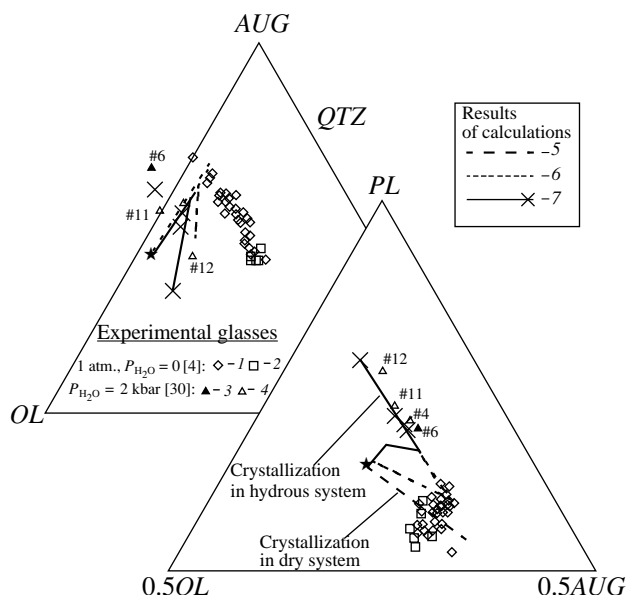


**Fig. 7.** Experimental ( $0.40 < Mg\# < 0.65$ ) and model melt compositions projected onto the pseudoternary diagrams *Ol–Aug–Qtz* and *Ol–Pl–Aug*. The asterisk denotes the composition of the starting high-alumina basalt (sample 79-35g); the projection method is after [33]. Phase associations: (1) *Ol + Pl + Aug + Mt + L*; (2) *Ol + Pl + Aug + Mt + Plg + L*; (3) *Ol + Mt + L*; and (4) *Ol + Pl + Aug + L*. Modeling was carried out at various initial  $H_2O$  content: (5)  $P = 2$  kbar,  $C_{H_2O} = 0$ ; (6)  $P = 2$  kbar,  $C_{H_2O} = 1$  wt %,  $P_{H_2O} < P$ ; (7)  $P = 2$  kbar,  $C_{H_2O} = 3.3$  wt %,  $P_{H_2O} < P$  (run #12). The asterisk denotes the composition of model melts at the moment of water saturation (Table 3).

placement of the *Ol–Cpx* phase boundary with plagioclase (*Ol–Cpx–Qtz* projection) toward the olivine apex under water-saturated conditions. The effect of depletion of hydrous melts in clinopyroxene accompanied by a considerable increase in plagioclase is more clearly demonstrated on the projection from the quartz apex (*Ol–Pl–Cpx* plane). Thus, the model compositional trends of a high-alumina melt are consistent with the well-known ideas on the delay of plagioclase crystallization and its accumulation in a residual melt in hydrous systems [30, 31, 34–36].

### CONCLUSIONS

(1) On the basis of experimental data on water solubility in basalt, andesite, and granite melts, we developed an empirical equation relating water concentration, temperature, pressure, and melt composition. The estimates of  $C_{H_2O}$  solubility obtained by this empirical equation (13) are in good agreement with values calculated using the Burnham [14] and Stolper [11, 16] models and yield an average error of 0.3 wt %  $H_2O$ .

(2) The empirical solubility equation was used to calculate  $H_2O$  concentration in quench glasses pro-

duced in 461 experiments on the melting of various rocks under water-saturated conditions and pressures of 1–10 kbar. The compositions of these glasses were grouped according to the presence of a particular mineral on the liquidus, which allowed us to accumulate data sets representing the temperatures of plagioclase–melt, pyroxene–melt, and olivine–melt equilibria. Proceeding from these data, the correction coefficients for the minerals of the basaltic system were calculated (Table 2), which account for the differentiated depression of the liquidus temperature due to the presence of water.

(3) These correction coefficients compose the empirical basis for the development of the hydrous version of the COMAGMAT model [4], with which phase equilibria can be calculated during the crystallization of water-bearing basaltic magmas.

The approach proposed in this paper is only the first step in the creation of a consistent computer model for the calculation of phase equilibria under hydrous conditions. This step does not account for the influence of water on the composition of minerals (primarily, plagioclase) or for possible crystallization of amphibole. The role of water during the crystallization of iron oxide phases is also little understood [13]. These questions are subjects for further investigations.

### ACKNOWLEDGMENTS

The authors thank V.N. Anfilogov for discussing the materials presented here. This work was supported by the Russian Foundation for Basic Research, project nos. 96-05-64231 and 96-07-89054.

### REFERENCES

1. Kinzler, R.J. and Grove, T.L., Primary Magmas of Mid-Ocean Ridge Basalts: 1. Experiments and Methods, *J. Geophys. Res.*, 1992, vol. 97, no. B5, pp. 6885–6906.
2. Nielsen, R.L., The Theory and Application of a Model of Open Magma System Processes, *Modern Methods of Igneous Petrology: Understanding Magmatic Processes*, *Rev. Mineral.*, 1990, vol. 24, pp. 65–106.
3. Ghiorso, M.S. and Sack, R.O., Chemical Mass Transfer in Magmatic Processes: IV. A Revised and Internally Consistent Thermodynamic Model for the Interpolation and Extrapolation of Liquid–Solid Equilibria in Magmatic Systems at Elevated Temperatures and Pressures, *Contrib. Mineral. Petrol.*, 1995, vol. 119, pp. 197–212.
4. Ariskin, A.A., Frenkel, M.Ya., et al., *A Fortran Program to Model Magma Differentiation Processes*, *Comput. Geosci.*, 1993, vol. 19, pp. 1155–1170.
5. Ariskin, A.A., Barmina, G.S., Ozerov, A.Yu., and Nielsen, R.L., Genesis of the High-Alumina Basalts of the Klyuchevskoi Volcano, *Petrologiya*, 1995, vol. 3, no. 5, pp. 496–521.
6. Frenkel, M.Ya., Yaroshevskii, A.A., Ariskin, A.A., et al., *Dinamika vnutrikamernoii differentsiatsii bazitovykh magm* (Dynamics of the Intrachamber Differentiation of Basic Magmas), Moscow: Nauka, 1988.

7. Yoder, H.S. and Tilley, C.E., Origin of Basalt Magmas, *J. Petrol.*, 1962, vol. 3, no. 3, p. 220.
8. Meshalkin, S.S., Ariskin, A.A., Barmina, G.S., Nikolaev, G.S., and Al'meev, R.R., Development of an Experimental Database on Melt–Crystal Equilibria in Igneous Rocks: INFOREX System (Version 3.0), *Geokhimiya*, 1996, no. 2, pp. 2–8.
9. Kushiro, I., Partial Melting of Mantle Wedge and Evolution of Island Arc Crust, *J. Geophys. Res.*, 1990, vol. 95, no. B10, pp. 15 929–15 939.
10. Luhr, J.F., Experimental Phase Relations of Water- and Sulfur-saturated Arc Magmas and the 1982 Eruptions of El Chichon Volcano, *J. Petrol.*, 1990, vol. 31, pp. 1071–1114.
11. Dixon, J.E., Stolper, E.M., and Holloway, J.R., An Experimental Study of Water and Carbon Dioxide Solubilities in Mid-Ocean Ridge Basaltic Liquids, *J. Petrol.*, 1995, vol. 36, pp. 1607–1646.
12. Holloway, J.R. and Blank, J.G., Application of Experimental Results to C–O–H Species in Natural Melts, *Volatiles in Magmas*, *Rev. Mineral.*, 1994, vol. 30, pp. 187–230.
13. Sisson, T.W. and Grove, T.L., Temperatures and H<sub>2</sub>O Contents of Low-MgO High-Alumina Basalts, *Contrib. Mineral. Petrol.*, 1993, vol. 113, no. 2, pp. 167–184.
14. Burnham, C.W., The Importance of Volatile Constituents, *The Evolution of the Igneous Rocks*, Princeton: Princeton University Press, 1979, pp. 1077–1084.
15. Housh, T.B. and Luhr, J.F., Plagioclase–Melt Equilibria in Hydrous Systems, *Am. Mineral.*, 1991, vol. 76, pp. 477–492.
16. Stolper, E., The Speciation of Water in Silicate Melts, *Geochim. Cosmochim. Acta*, 1982, vol. 46, no. 12, pp. 2609–2620.
17. Burnham, C.W. and Davis, N.F., The Role of H<sub>2</sub>O in Silicate Melts: I. P–V–T Relations in the System NaAlSi<sub>3</sub>O<sub>8</sub>–H<sub>2</sub>O to 10 kilobars and 1000°C, *Am. J. Sci.*, 1971, vol. 270, pp. 54–79.
18. Burnham, C.W. and Davis, N.F., The Role of H<sub>2</sub>O in Silicate Melts: II. Thermodynamic and Phase Relations in the System NaAlSi<sub>3</sub>O<sub>8</sub>–H<sub>2</sub>O to 10 kilobars, 700 to 1000°C, *Am. J. Sci.*, 1974, vol. 274, pp. 902–940.
19. Burnham, C.W., Thermodynamics of Melting in Experimental Silicate–Volatile Systems, *Fortschr. Miner.*, vol. 52, pp. 101–118.
20. Burnham, C.W., Development of the Burnham Model for Prediction of the H<sub>2</sub>O Solubility in Magmas, *Volatiles in Magmas*, *Rev. Mineral.*, 1994, vol. 30, pp. 123–129.
21. Frazer, D.G., Thermodynamic Properties of Silicate Melts, *Thermodynamics in Geology*, Dordrecht, Holland, 1977, pp. 301–326.
22. Epel'baum, M.B., *Silikatnye rasplavy s letuchimi komponentami* (Silicate Melts with Volatile Components), Moscow: Nauka, 1980, p. 254.
23. Anfilogov, V.N. and Bobylev, I.B., Thermodynamic Analysis of Water Solution in Silicate Melts, *Geokhimiya*, 1985, no. 9, pp. 1277–1285.
24. McMillan, S.S. and Holloway, J.R., Water Solubility in Aluminosilicate Melts, *Contrib. Mineral. Petrol.*, 1987, vol. 97, pp. 320–332.
25. Silver, L. and Stolper, E., Water in Albitic Glasses, *Contrib. Mineral. Petrol.*, 1989, vol. 30, no. 3, pp. 667–709.
26. Hamilton, D.L., Burnham, C.W., and Osborn, E.F., The Solubility of Water and Effect of Oxygen Fugacity and Water Content on Crystallization in Mafic Magmas, *J. Petrol.*, 1964, vol. 5, pp. 21–39.
27. Kadik, A.A., Lebedev, E.B., and Khitarov, N.I., *Voda v magmaticheskikh rasplavakh* (Water in Igneous Melts), Moscow: Nauka, 1971, p. 210.
28. Lange, R.L. and Carmichael, I.S.E., Thermodynamic Properties of Silicate Liquids with Emphasis on Density, Thermal Expansion and Compressibility, *Modern Methods in Igneous Petrology: Understanding Magmatic Processes*, *Rev. Mineral.*, 1990, vol. 24, pp. 25–64.
29. Holtz, F., Behrens, H., Dingwell, D.B., and Johannes, W., H<sub>2</sub>O Solubility in Haplogranitic Melts: Compositional, Pressure, and Temperature Dependence, *Am. Mineral.*, 1995, vol. 80, no. 1/2, pp. 94–108.
30. Sisson, T.W. and Grove, T.L., Experimental Investigations of the H<sub>2</sub>O in Calc-Alkaline Differentiation and Subduction Zone, *Contrib. Mineral. Petrol.*, 1993, vol. 113, no. 2, pp. 143–166.
31. Mueller, R.F. and Saxena, S.K., *Chemical Petrology*, New York: Springer, 1977, p. 510.
32. Al'meev, R.R. and Ariskin, A.A., Calculating Water Solubility in Basalt and Andesite Melts at Pressures up to 10 kbar, *XIII Rossiiskoe soveshchanie po eksperimental'noi mineralogii. Tez. Dokl.* (Abstr. XIII Russian Symposium on Experimental Mineralogy), 1995, p. 126.
33. Tormey, D.R., Grove, T.L., and Bryan, W.B., Experimental Petrology of Normal MORB Near the Kane Fracture Zone: 22–25°N, Mid-Atlantic Ridge, *Contrib. Mineral. Petrol.*, 1987, vol. 96, pp. 121–139.
34. Kadik, A.A., Maksimov, A.P., and Ivanov, B.V., *Fiziko-khimicheskie usloviya kristallizatsii i genezis andezitov* (Physicochemical Conditions of Crystallization and Genesis of Andesites), Moscow: Nauka, 1986, p. 158.
35. Yoder, H.S.J., Diopside–Anorthite–Water at Five and Ten Kilobars and its Bearing on Explosive Volcanism, *Year Book–Carnegie Inst. Washington*, 1965, vol. 64, pp. 82–89.
36. Grove, T.L. and Baker, M.B., Phase Equilibrium Controls on the Tholeiitic Versus Calc-Alkaline Differentiation Trends, *J. Geophys. Res.*, 1984, vol. 89, pp. 3253–3274.